PERGAMON

International Journal of Solids and Structures 40 (2003) 4071–4090

INTERNATIONAL JOURNAL OF SOLIDS and STRUCTURES

www.elsevier.com/locate/ijsolstr

Nonlinear parameter identification of models for masonry

Renata Morbiducci *

Department of Structural and Geotechnical Engineering, University of Genova, Via Montallegro 1, Genova 16145, Italy

Received 29 October 2001; received in revised form 7 March 2003

Abstract

This paper investigates the parameter estimation problem for brick masonry models. An identification procedure is proposed in which the uncertainties of known parameters and/or errors of measurements are its elements of distinction. The minimization process of the discrepancies between experimental data and theoretical measurements takes place by means of a first order iterative method. The identification procedure is applied to two different problems: the calibration of an interface model for brick–mortar joint in its functional form through monotonic experimental tests; to evaluate the unknown parameters of a continuum model for brick masonry walls in its non-holonomic form by means of in-plane cyclic shear–compression test of masonry panels. The general framework of the non-linear estimate methodology, the parameter identification problems and the numerical results are presented.

Keywords: Parameter identification; Brick masonry; Interface model; Continuum model

1. Introduction

Model calibration is an important phase of the theoretical investigation of the mechanical behavior of materials and structures. Constitutive models for anisotropic materials, such as masonry, contain several material parameters that have to be quantified on the basis of experimental tests. Nevertheless, these parameters cannot be determined explicitly from standard or sophisticated experimental tests because of material heterogeneity and the simultaneous or sequential estimation through parameter identification method must be carried out. It is well known that a parameter identification problem consists of the optimal estimate of the parameters through an inverse process in which the deviations between experimental and theoretical measurements are minimized. Several issues emerge in this kind of process such as the optimal design of experiments, linear or non-linear programming and methods of error treatment in the optimization process or error estimate in the identified parameters (Bard, 1974; Sorenson, 1980; Luenberg, 1989; Federov and Hackl, 1997).

Although brick masonry is one of the most ancient and widespread composite materials, remarkable difficulties are still encountered in the formulation of adequate constitutive models due to its heterogeneity

* Tel.: +39-10-353-2942; fax: +39-10-353-2534.
E-mail address: morbiducci@diseg.unige.it (R. Morbiducci).

0020-7683/03/$ - see front matter © 2003 Elsevier Science Ltd. All rights reserved.
doi:10.1016/S0020-7683(03)00170-7

and anisotropy. In such formulations a preliminary experimental and theoretical characterization of each component, brick units and mortar, and of the interfaces must precede the definition of the global constitutive equations. This work gives attention to the calibration problem of masonry constitutive models considering the in-plane response either of the mortar–brick interface or of masonry walls under the horizontal actions representative of the seismic ones.

This paper is organized as follows: In Section 2 some particular experimental and theoretical aspects of the response of the mortar–brick interface and of in-plane loaded masonry walls are analyzed to introduce some topics in the current research about masonry. In Section 3 two different models for masonry are presented, an interface model for brick–mortar joints and a continuum model for brick masonry walls (Gambarotta and Lagomarsino, 1997a,b). The two models have similar formulations and they both examine the inelastic mechanisms induced by damage and frictional sliding. However they apply to problems with different complexities. The interface model concerns the local problem to analyze the brick–mortar joint response considering few degree of freedom; while the continuum model concerns the evaluation of the lateral response of in-plane loaded brick masonry shear walls considering finite element simulations with a large number of degrees of freedom.

In Section 4 the theoretical aspects of the non-linear parameter identification problem are discussed, three different estimate approaches are considered, the presence of the known parameters uncertainty and/or of the errors in measurements characterizes them. Furthermore, an inverse procedure for the calibration of the masonry models is proposed.

The aim of Section 5 is to verify the efficiency of the identification procedure proposed in the previous section considering the different complexity of the masonry models. In the estimate process for the interface model the constitutive equations are in holonomic form that implies a remarkable speed in computation. In the case of the continuous model the equations are in the non-holonomic form performing finite element analyzes and estimate processes in to high-dimensional parameter space.

2. In-plane response of brick masonry: experimental tests and mechanical models

Masonry is a composite material, whose mechanical response is non-linear even at low stress levels. A high number of factors affect its in-plane behavior, among which are the mechanical and geometrical properties of brick units and mortar, the characteristics of their interfaces and the geometrical arrangement of the masonry. Experimental investigation of brick masonry is usually carried out at local and global level: local tests consider the single components (mortar, brick units and their interfaces), while global tests involve the masonry composite material in the form of simple assemblages or structural elements.

Several local tests are possible, but for the purpose of present work, only shear tests will be considered. The shear test on brick–mortar joints is typically used, because the mortar joints are the predominant planes of weakness. This kind of test is carried out on small assemblages of brick units and mortar bed joints subject to horizontal and vertical loads (Aktinson et al., 1989; Van Der Pluijm, 1993; Binda et al., 1994; Manzouri et al., 1995): the initial response is linear, then it becomes non-linear up to the attainment of the limit strength; when acting under displacement control this test is characterized by a stable strain-softening phase (Fig. 1) in which the tangential stress progressively decreases to obtain a residual shearing strength of the broken interface between bricks and mortar joint. Such response is mainly due to the final phase characterized by frictional sliding between bricks and it allows a complete description of the mechanical response of the interfaces.

The shear response of brick–mortar joints has been simulated by several interface models taking into account the degradation processes which take place when opening and frictional sliding are activated (e.g., Lofti and Shing, 1994; Gambarotta and Lagomarsino, 1997a; Lourenço and Rots, 1997). The calibration of these models is usually difficult, since some of the parameters have to be determined from indirect

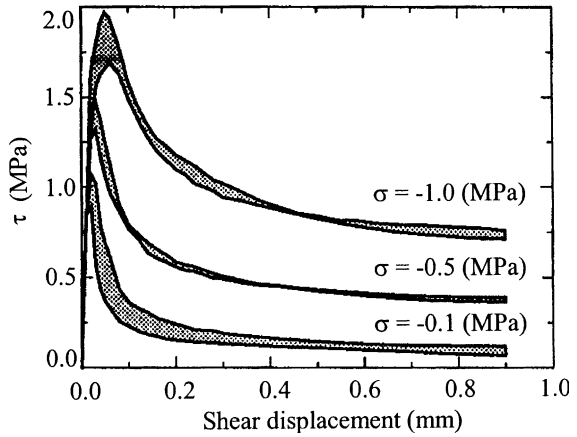

Fig. 1. Experimental results by the direct shear test (Van Der Pluijm, 1993).

measurements. Such inverse processes can be facilitating when monotonic response is considered and the constitutive equations are reduced to their holonomic form.

A useful test for masonry as composite material is the cyclic shear–compression test of masonry panels. This test is meaningful to investigate the seismic behavior of masonry shear walls. Several researchers adopted this experimental method among whom Anthoine et al. (1995), who tested two brick masonry walls with different slenderness. The results of the quasi-static loading pointed out the effect of the height/width ratio on the behavior of the walls (see Fig. 2). The *low wall* exhibited a limit lateral strength followed by a post-peak behavior with a significant stiffness degradation and increase of dissipation. The cyclic response of the *high wall* pointed out the presence of an overturning mechanism with low degradation and dissipation.

Several continuum models for masonry have recently been proposed based on homogenization techniques of heterogeneous material to take into account the effective geometry of the investigated elements (e.g., Pande et al., 1989; Anthoine, 1995; Papa, 1996; Gambarotta and Lagomarsino, 1997b; Luciano and Sacco, 1997; Lourenço et al., 1998). The constitutive equations of such models are worded in the non-holonomic form. Moreover, the integration of these kind of constitutive equations needs a finite element modeling of the two-dimensional domain. The calibration of such models is more complex than the

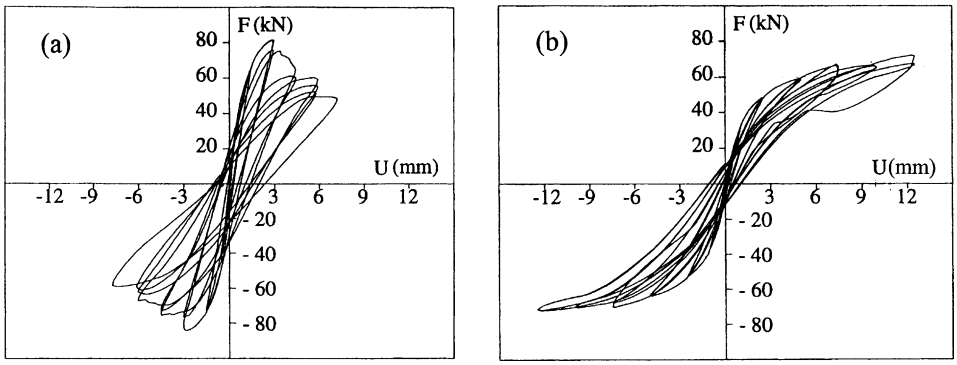

Fig. 2. Experimental results from shear tests superimposed on uniform compression on brick masonry walls of different height/width ratio: (a) low wall $h = 135$ cm, $b = 100$ cm; (b) high wall $h = 200$ cm, $b = 100$ cm.

parameter estimation of the interface models. Besides the large number of parameters and the large computational efforts for the parameter estimates, there are others factors, which affect the goodness of estimate. For instance the efficiency of F.E. analysis or the difficulty of making a reliable a posteriori analysis of identification process.

3. Damage models for masonry

An interface model for brick–mortar joint (Gambarotta and Lagomarsino, 1997a) and a continuum model for masonry (Gambarotta and Lagomarsino, 1997b) are considered in order to simulate, respectively, the experimental tests on brick–mortar interfaces and on masonry walls subjected to cyclic loads.

The interface model, based on damage mechanics takes into account the effects of compression on joints in the damage and failure processes, the strain-softening response and the cyclic shear response superimposed on normal compressive stress. The constitutive equations for brick masonry are obtained through a homogenization procedure involving the local damage model.

In the following part the characteristics of the continuum and interface models are discussed in order to explain the meaning of each parameter, while one is referred to Gambarotta and Lagomarsino (1997a,b) for a complete exposition of the models.

The continuum model for in-plane loaded brick masonry is obtained on the hypothesis of plane stress condition. The brick masonry is assumed as a stratified medium made up of the bed mortar joint layer and the brick units layer in which the mortar head joints are neglected. The constitutive model is obtained homogenizing the two different layers and taking into account the inelastic mechanisms; the mean strain $\underline{\varepsilon} = \{\varepsilon_1 \ \ \varepsilon_2 \ \ \gamma\}^{\mathrm{T}}$, where 1 and 2 are the directions parallel and normal to the mortar bed joints, is given by

$$\underline{\varepsilon} = \underline{K}_M \underline{\sigma} + \eta_m \underline{\varepsilon}_m^* + \eta_b \underline{\varepsilon}_b^*, \tag{1}$$

where $\underline{K}_M$ is the elastic orthotropic compliance matrix of the masonry and depends on four elastic constants $(E_{M1}, E_{M2}, G_M, \nu_{M12})$; $\underline{\sigma} = \{\sigma_1 \ \ \sigma_2 \ \ \gamma\}^{\mathrm{T}}$ is the mean stress; $\underline{\varepsilon}_m^* = \{0 \ \ \varepsilon_m \ \ \gamma_m\}^{\mathrm{T}}$ and $\underline{\varepsilon}_b^* = \{0 \ \ \varepsilon_b \ \ \gamma_b\}^{\mathrm{T}}$ are the inelastic strains in mortar joint and bricks respectively; η_m and η_b are the mortar and brick volume fractions, respectively.

The inelastic mechanisms in the bed joints, which locally characterize the interface model, describe the failure in the mortar and the decohesion in the contact zone between mortar and brick. The extension ε_m and the sliding γ_m due to the inelastic mechanisms are assumed linearly dependent on the applied stress as follows:

$$\varepsilon_m = c_{mn} \alpha_m H(\sigma_2) \sigma_2, \tag{2a}$$

$$\gamma_m = c_{mt} \alpha_m (\tau - f), \tag{2b}$$

where c_{mn} and c_{mt} are the extensional and tangential inelastic compliance parameters, α_m is the mortal damage variable, $H(\cdot)$ is the Heaviside function which takes into account the unilateral response of the joint, σ_2 and τ are the resolved stresses on the mortar bed joint and f represents the friction in the mortar–brick interface and reduces the sliding mechanism.

The other contributions of inelastic strain $\underline{\varepsilon}_b^*$ consider the effects of the vertical compression on the masonry and of the shear stresses on the brick units; such effects are expressed in terms of a damage variable α_b:

$$\varepsilon_b = c_{bn} \alpha_b H(-\sigma_2) \sigma_2, \tag{3a}$$

$$\gamma_b = c_{bt} \alpha_b \tau, \tag{3b}$$

where c_{bn} and c_{bt} are inelastic compliance parameters of the bricks, α_b is the brick damage variable.

When the internal variables α_m, α_b and the sliding level γ_m are known, Eqs. (1)–(3) supply the inelastic strains for a given stress state. The evolution of variables are obtained defining three limit conditions in which Y_m the density of damage energy release rate in mortar joint, the friction f and Y_b the density of damage energy release rate in bricks are introduced, respectively. These limit conditions must be satisfied during the loading process:

$$\begin{aligned} &\phi_s = |f| + \mu\sigma_2 \leqslant 0, \\ &\phi_{dm} = Y_m - \mathscr{R}_m = \tfrac{1}{2}c_{mn}\sigma_2^2 + \tfrac{1}{2}c_{mt}\tau^2 - \mathscr{R}_m(\alpha_m) \leqslant 0, \\ &\phi_{db} = Y_b - \mathscr{R}_b = \tfrac{1}{2}c_{bt}\tau^2 - \mathscr{R}_b(\alpha_b) \leqslant 0. \end{aligned} \tag{4a–c}$$

Eq. (4a) is based on linear Coulomb frictional law and it involves, beyond the friction f, the normal stress σ_2 on the joint plan by means of the friction coefficient μ. In (4b) and (4c) the mortar joint and brick unit toughness functions $\mathscr{R}_m(\alpha_m)$ and $\mathscr{R}_b(\alpha_b)$ are introduced, respectively, depending on α_m, α_b (damage variables) and $\underline{\beta}_m$, $\underline{\beta}_b$ (model parameters). These parameters control the post-peak responses; hence for the mortar joint and brick unit can be defined as $\mathscr{R}_z(\alpha_z, \underline{\beta}_z)$, $(z = m, b)$.

The masonry failure domain is obtained through the intersection of the mortar joint and the brick failure domains. Finally c_{mn}, c_{mt}, c_{bn} and c_{bt} can be correlated to some parameters which can be measured directly by experimental tests.

In the previous discussion concerning the homogenized constituent materials of the masonry the parameters of the elastic and inelastic response were introduced. In Table 1, they are summarized, distinguishing the quantities of the different phases of the response.

In order to evidence the peculiar aspects of the estimate problem for the interface model, some remarks will be added when compression and shear stress act on the joint. In this case the model is reduced to the shear response and it does not include the brick units damage.

The sliding response of the model is characterized by three different phases (see Fig. 3), each depending on different sets of parameters shown in Table 2. The corresponding equations of three different phases are written replacing the damage variable α_m with its expression in terms of material parameters. Moreover, in the applications which will be shown, the toughness $\mathscr{R}_m$ is assumed equal to

$$\mathscr{R}_m(\alpha_m) = \begin{cases} \mathscr{R}_{mc}\alpha_m & 0 < \alpha_m < 1, \\ \mathscr{R}_{mc}\alpha_m^{-\beta_m} & \alpha_m \geqslant 1, \end{cases} \tag{5}$$

where $\mathscr{R}_{mc}$ is the maximum value of the toughness corresponding to the limit state, $\alpha_m = 1$ (representative of the mortar joint failure).

$$\gamma = \frac{\tau}{G_m}, \tag{6}$$

$$\gamma = \frac{\tau}{G_m} + c_{mt}\frac{(\tau - \mu|\sigma_2|)^3}{\tau_m^2}, \tag{7}$$

Table 1
Parameters of the continuum damage model

Branch phase	Parameters	Number of parameters
Elastic (OA)	E_{M1}, E_{M2}, G_M, ν_{M12}	4
Pre-peak (AB)	μ, σ_{mr}, τ_m, σ_{br}, τ_{br}, c_{mt}, c_{bn} (+ phase OA)	4 + 7 = 11
Post-peak (BC)	β_m, β_b (+ phase OA + phase AB)	11 + 2 = 13

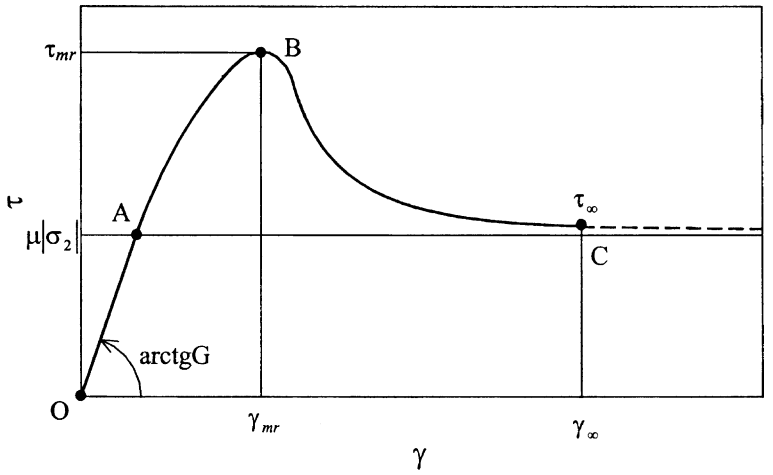

Fig. 3. Model response of the mortar–brick joint to shearing strain superimposed on constant compressive stress.

Table 2
Parameters of the interface model

Branch phase	Parameters	Number of parameters
Elastic (OA)	G_m	1
Pre-peak (AB)	G_m, c_{mt}, μ, τ_m (+ phase OA)	1 + 3 = 4
Post-peak (BC)	G_m, c_{mt}, μ, τ_m, β_m (+ phase OA + phase AB)	4 + 1 = 5

$$\gamma = \frac{\tau}{G_m} + c_{mt}\left(\frac{\tau_m}{\tau - \mu|\sigma_2|}\right)^{2/\beta_m}(\tau - \mu|\sigma_2|). \tag{8}$$

The model response is elastic until point A (see Fig. 3), when the limit state $\phi_s = |\tau| + \mu\sigma_2 = 0$, that is until the shear stress τ on the joint plane is less than the internal friction f. In this phase the shearing strain in the joint is given by (6), this is a linear relationship ruled by the tangential elastic modulus G_m. Once such limit is reached (branch AB) the response is not linear and ruled by (7). In this phase the model takes into account the appearance and the propagation of the cracks in the mortar joint. In Eq. (7) the inelastic compliance parameter of the joint c_{mt}, the friction coefficient μ and the joint cohesion τ_m are involved, as well as the tangential elastic modulus G_m. The model response, after reaching the shear strength τ_{mr} (limit point B, branch BC), is characterized by a strain-softening phase that is governed by (8). In this phase the parameter β_m controls the slope of the post-peak branch and the shear stress tends asymptotically to the limit value τ_∞. This limit value represents the residual strength due to the friction.

4. Non-linear parameter estimation

Consider an experimental test performed on M specimens to estimate the unknown parameters of a constitutive model or a mechanical model. Let Q be the number of sensors used to record the experimental data. The sensors are localized by their coordinates $\underline{X} = [x_{qi}]$ (where $q = 1, 2, \ldots, Q$ denotes a sensor; $i = 1, 2, 3$ identifies the reference axes (O, x_1, x_2, x_3)). Let N be the number of readings in sequential times $\underline{t} = \{t_n\}$ $(n = 1, 2, \ldots, N)$ for each sensor. The input data of experimental test at the time t_n are defined as $\underline{\bar{\xi}}_n = [\bar{\xi}_{hn}]$ $(h = 1, 2, \ldots, H < Q)$ and their components represent the variables associated with the H selected

sensors. The H sensors are localized by their coordinates $\underline{X}^I = [x^I_{hi}]$ (a subset of $\underline{X}$). Likewise the output data of an experimental test at time t_n are defined as $\underline{\overline{\psi}}_n = [\overline{\psi}_{rn}]$ $(r = H+1, H+2, \ldots, Q)$ and their components represent the variables associated with the $(Q-H)$ selected sensors. Analogously the $(Q-H)$ sensors are localized by their coordinates $\underline{X}^O = [x^O_{ri}]$ (a subset of $\underline{X}$).

Then consider a theoretical model where a p-dimensional vector of unknown parameters $\underline{\theta} = \{\theta_p\}$ $(p = 1, 2, \ldots, P)$ and an l-dimensional vector of known parameters $\underline{b} = \{b_l\}$ $(l = 1, 2, \ldots, L)$ may be distinguished. The model takes the general functional form:

$$\underline{\psi} = \underline{f}(\underline{\xi}, \underline{\theta}, \underline{b}), \tag{9}$$

where $\underline{\xi} = \{\xi_h\}$ $(h = 1, 2, \ldots, H < Q)$ are the independent variables and correspond to the input data of experimental test $\underline{\overline{\xi}}_n$; $\underline{\psi} = \{\psi_r\}$ $(r = H+1, H+2, \ldots, Q)$ are the dependent variables and agree with the output data of experimental test $\underline{\overline{\psi}}_n$; $\underline{f} = \{f_r\}$ is an r-dimensional vector of functions.

When the theoretical model is applied to simulate real process, i.e. an experimental test, the theoretical variables $\underline{\xi}$ are replaced by the experimental input $\underline{\overline{\xi}}_n$ (relative to the observed test), the values of known parameters $\underline{b}$ are substituted and it is necessary to estimate the unknown parameters. The elements of $\underline{b}$ are measured by ad hoc experimental tests or they are estimated in previous identification problems. Whereas the values of parameters $\underline{\theta}$ are not known and can be evaluated by an estimate process. That is they are determined by an inverse problem that can be considered as a problem in which $\underline{\theta}$ are identified by minimizing a specific measure of performance. In this case model (9) takes the form

$$\underline{\psi}_n = \underline{f}(\underline{\overline{\xi}}_n, \underline{\theta}, \underline{b}). \tag{10}$$

The aim of an identification problem is the optimal estimate $\underline{\hat{\theta}}$ of unknown model parameters taking into account uncertainties which might exist in this type of problem. These uncertainties are due to several factors, experimental errors, the estimate method and theoretical model quality. Assuming that model errors are negligible, in the following part of the section the other factors are analyzed.

In general, experimental test is affected with systematic and random errors. In this work it is assumed that the former are negligible and the latter is characterized by a Gaussian distribution. The recorded data of M specimens are used to evaluate the expected value and the variance of the studied experimental test. It ensues that the $\underline{S}_n$ covariance matrix of the measurements ($[(Q-H)\times(Q-H)]$) at time t_n is defined as

$$\underline{S}_n = E\left[\delta\underline{\overline{\psi}}_n \delta\underline{\overline{\psi}}_n^{\mathrm{T}}\right], \tag{11}$$

where $\delta\underline{\overline{\psi}}_n = \underline{\overline{\psi}}_n - E[\underline{\overline{\psi}}_n]$, $E[\underline{\overline{\psi}}_n]$ is the expected value of $\underline{\overline{\psi}}_n$. In (11) $\underline{\overline{\psi}}_n$ experimental output are present only, because the errors of $\underline{\overline{\xi}}_n$ experimental input are considered negligible.

In addition to the experimental errors, the estimate problem will also be affected by uncertainties of known parameters; in fact these parameters are evaluated in a previous estimate or directly through experimental tests. To define the characteristics of this random component some general considerations are necessary. Let the residual be $\underline{e}_n$, at time t_n, the vector whose elements are the difference between the experimental components of the vector $\underline{\overline{\psi}}_n$ and the corresponding theoretical components of the vector $\underline{\psi}_n$ (Bard, 1974):

$$\underline{e}_n = \underline{\overline{\psi}}_n - \underline{\psi}_n. \tag{12}$$

Assuming $\underline{\overline{\psi}}_n$, $\underline{\psi}_n$ and $\underline{e}_n$ to be normally distributed (Fadale et al., 1995), $\underline{V}_n$ the covariance matrix of residual $\underline{e}_n$ ($[(Q-H)\times(Q-H)]$) is given by

$$\underline{V}_n = E\left[\{\underline{e}_n - E[\underline{e}_n]\}\{\underline{e}_n - E[\underline{e}_n]\}^{\mathrm{T}}\right] = E\left[\delta\underline{\psi}_n \delta\underline{\psi}_n^{\mathrm{T}}\right] + E\left[\delta\underline{\overline{\psi}}_n \delta\underline{\overline{\psi}}_n^{\mathrm{T}}\right], \tag{13}$$

where $\delta\underline{\psi}_n = \underline{\psi}_n - E[\underline{\psi}_n]$.

The second part of (13) tallies with (11) which is the covariance due to the experimental noise; while the first part is the covariance due to the statistical nature of the known parameters $\underline{b}$ and is given by Fadale et al. (1995):

$$E\left[\delta\underline{\psi}_n \delta\underline{\psi}_n^{\mathrm{T}}\right] = \underline{\Theta}_n \underline{G} \underline{\Theta}_n^{\mathrm{T}}, \tag{14}$$

where $\underline{\Theta}_n$ is the sensitivity matrix at time t_n, which is defined by (Sorenson, 1980):

$$\underline{\Theta}_n = \frac{\partial \underline{f}(\bar{\underline{\xi}}_n, \underline{\theta}, \underline{b})}{\partial \underline{b}} \tag{15}$$

and $\underline{G}$ is the covariance matrix of known parameters $\underline{b}$, in terms of uncertainties (the diagonal terms) and of the correlation between the parameters (the non-diagonal terms). Thus Eq. (13) is written as

$$\underline{V}_n = \underline{\Theta}_n \underline{G} \underline{\Theta}_n^{\mathrm{T}} + \underline{S}_n. \tag{16}$$

The matrix in the first part of (16) represents the uncertainties of $\underline{b}$.

In the following part of section three different estimate methods are discussed in which the uncertainty of known parameters and/or the errors of measurements are their elements of distinction.

An approach to account for both types of uncertainties in the identification process is the search for a maximum of the conditional probability density function $f(\underline{e}|\underline{\theta})$, in which random vector coincides with the residual $\underline{e}$, given the measurements of $\underline{\theta}$ (Sorenson, 1980):

$$f(\underline{e}|\underline{\theta}) = \left[(2\pi)^{(Q-H)N} \prod_{n=1}^{N} \mathrm{Det}(\underline{V}_n)\right]^{-1/2} \times \exp\left[\sum_{n=1}^{N} -\frac{1}{2} \underline{e}_n^{\mathrm{T}} \underline{V}_n^{-1} \underline{e}_n\right]. \tag{17}$$

When experimental data noise is assumed to be independent of unknown parameters, the estimate approach can reduce to maximizing the corresponding logarithmic function of (17) (Fadale et al., 1995):

$$J(\underline{\theta}, \underline{b}) = -2 \ln f(\underline{e}|\underline{\theta}) = \sum_{n=1}^{N} \ln[\mathrm{Det}(\underline{V}_n)] + \sum_{n=1}^{N} \underline{e}_n^{\mathrm{T}} \underline{V}_n^{-1} \underline{e}_n. \tag{18}$$

If only the experimental uncertainties are present in logarithmic function the identification criterion coincides with the maximum likelihood approach and (18) will be (Sorenson, 1980):

$$L(\underline{\theta}) = -2 \ln f(\overline{\underline{\psi}}|\underline{\theta}) = \sum_{n=1}^{N} \underline{e}_n^{\mathrm{T}} \underline{S}_n^{-1} \underline{e}_n. \tag{19}$$

Finally, the estimate criterion coincides with the weighted least squares method if the information on errors are only qualitative and inserted with weight factors:

$$\Phi(\underline{\theta}) = \sum_{m=1}^{M} \sum_{n=1}^{N} \underline{e}_{mn}^{\mathrm{T}} \underline{W}_{mn} \underline{e}_{mn}, \tag{20}$$

where $\underline{W}_{mn}$ is the matrix of weight factors, at time t_n considering the m specimen. The mean of such matrix can be reassumed in the following manner, the various quantities $\overline{\psi}$ in the residuals $\underline{e}_{mn}$ may represent entities measured on different scales. It clearly makes no sense to sum together squares of numbers of different orders of magnitude. Moreover, some observations may be known to be less reliable than others. The chosen solution to both of these problems is to assign a non-negative weight factor $\underline{W}_{mn}$ to each $\underline{e}_{mn}$. In (20) the index of specimens number m ($m = 1, 2, \ldots, M$) is present, because the number of experimental data it must appear directly in the objective function.

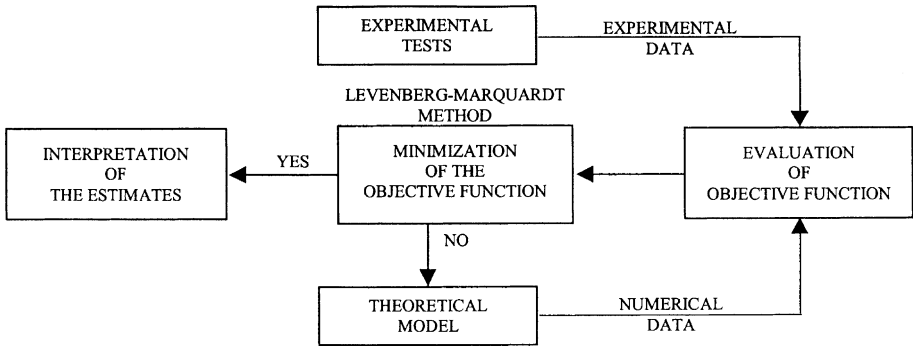

Fig. 4. Logical scheme to identify model parameters.

❑ 1 Selection of first attempt vector of parameters $\underline{\theta}_k$

❑ 2 Evaluation of $\underline{\theta}_{k+1}$

(a) Objective function approximation through a second order Taylor's series

$$\Phi(\underline{\theta}) \cong \Phi(\underline{\theta}_k) + \underline{\nabla}\Phi(\underline{\theta}_k)(\underline{\theta} - \underline{\theta}_k) + \tfrac{1}{2}(\underline{\theta} - \underline{\theta}_k)^T \underline{\widetilde{B}}(\underline{\theta}_k)(\underline{\theta} - \underline{\theta}_k)$$

(b) Imposition of minimum condition of $\Phi(\underline{\theta})$

$$\underline{\nabla}\Phi(\underline{\theta}) \cong \underline{\nabla}\Phi(\underline{\theta}_k) + \underline{\widetilde{B}}(\underline{\theta}_k)(\underline{\theta} - \underline{\theta}_k) = 0$$

(c) Computation of partial numerical derivatives of $\underline{g}_k$ and $\underline{\widetilde{B}}_k$ with respect to $\underline{\theta}_k$

(d) Evaluation of $\underline{\theta}_{k+1}$

$$\underline{\theta}_{k+1} = \underline{\theta}_k - (\varepsilon_k \underline{I} + \underline{\widetilde{B}}_k)^{-1} \underline{g}_k \text{ (when } k = 1,\ 0 < \varepsilon_k < 1)$$

❑ 3 Evaluation of $\underline{\psi}\big|_{\underline{\theta}=\underline{\theta}_{k+1}}$

❑ 4 Evaluation of $\Phi(\underline{\theta}_{k+1})$

❑ 5 Iterations control

If $\Phi(\underline{\theta}_{k+1}) > \Phi(\underline{\theta}_k)$

$\varepsilon_{k+1} = 10\,\varepsilon_k$, go to 2

if $\Phi(\underline{\theta}_{k+1}) < \Phi(\underline{\theta}_k)$

$\varepsilon_{k+1} = 0.1\,\varepsilon_k$,

if $|\Phi_{k+1} - \Phi_k| > tol.1$ and $\|\theta_{k+1} - \theta_k\| > tol.2$ go to 2

stop, convergence achievement

Fig. 5. Iterative algorithm for objective function minimization.

The aforementioned estimate criteria are applicable to unconstrained and to constrained non-linear identification problems and coincide with the objective function of the identification procedure proposed in this work. The first phase of the procedure (see Fig. 4) consists of the comparison of experimental data with the numerical results evaluated with a theoretical model. For such comparison, an objective function is defined following one of the above mentioned criteria. Since the identification problems in the present study are non-linear, the minimization of the function is based on an iterative method, a Levenberg–Marquardt method characterized by use of the Gauss–Newton matrix as a simplified Hessian matrix (Luenberg, 1989; Press et al., 1992). In this method, the parameter estimation in $(k+1)$th iteration can be written as

$$\underline{\theta}_{k+1} = \underline{\theta}_k + \underline{d}_k, \tag{21}$$

where

$$\underline{d}_k = -(\varepsilon_k \underline{I} + \widetilde{\underline{B}}_k)^{-1} \underline{g}_k, \tag{22}$$

in which ε_k is a non-negative parameter and the gradient $\underline{g}_k$ and the Gauss–Newton matrix $\widetilde{\underline{B}}_k$ are dependent to the different estimate criteria. The termination of iterative process occurs as a result of the satisfaction of the following criteria: an iterative estimate is terminated when the change in value of objective function for successive steps becomes less than a prescribed tolerance value $\Phi_{k+1} - \Phi_k < \text{tol.1}$, together with the condition that the distance between successive trial points vanishes. The latter implies that the search terminates when the magnitude of the steps becomes less than prescribed tolerance, $\|\underline{\theta}_{k+1} - \underline{\theta}_k\| < \text{tol.2}$.

It is worth noting that for the evaluation of $\underline{g}_k$ and of $\widetilde{\underline{B}}_k$ first partial derivatives are only necessary, which can be computed numerically. In Fig. 5 the numerical algorithm to minimize the generic objective function $\Phi(\underline{\theta})$ is shown.

5. Numerical examples

The identification procedure is applied to two different problems: the calibration of an interface model for brick–mortar joint in its functional form through monotonic experimental tests; the evaluation of the unknown parameters of a continuum model for brick masonry walls in its non-holonomic form by means of in-plane cyclic shear–compression test of masonry panels.

5.1. Non-linear estimate of holonomic interface model

When the brick–mortar joint is subjected to tangential loads superimposed on vertical compressive stress, the constitutive equations of the aforementioned interface model are governed by the parameter vector $\underline{\theta} = \{G_m \;\; c_{mt} \;\; \mu \;\; \tau_m \;\; \beta_m\}^{\mathrm{T}}$ (see (6)–(8)). Although these parameters are related to the physical properties of mortar joints some of them cannot be determined directly from simple experimental tests. Calibration of the model thus takes place through the inverse processes described in Section 4 (see Fig. 5).

The *shear tests* are chosen as *experimental tests*. These tests are performed according to the RILEM Recommendation 127 MS.B4 (Binda et al., 1994). The specimens consist of prisms made with three units (bricks) and two mortar bed joints (triplet test). These tests were carried out by applying a monotonically increasing displacement to the central unit, parallel to the bed joints (Fig. 6a). Four sets of specimens were tasked. They were subjected to normal compression stresses of 0.12, 0.4, 0.8 and 1.25 MPa, respectively. Each set consisted of three specimens subjected to the same compression stress. During each test, 10 LVDTs (linear variable displacement transducers) were used to measure horizontal and vertical

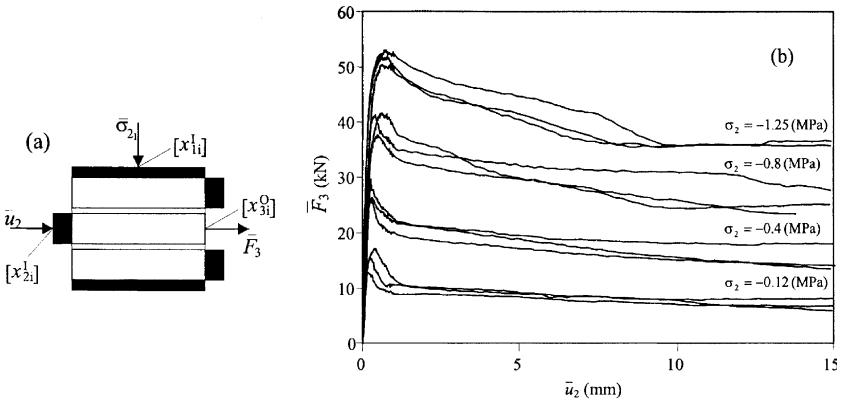

Fig. 6. Shear response of mortar joints: (a) the shear triplet test apparatus; (b) shear load vs. shear displacement curves under different vertical compressive loads (0.12, 0.4, 0.8, 1.25 MPa), (Binda et al., 1994).

displacements in different parts of the specimens. For parameter identification the following are considered as input: the measurements recorded by the sensor identified by its position $[x^I_{1i}]$ (where it is reminded that the first index indicates the number of the sensor and i identifies the coordinates in a Cartesian reference) from which the constant normal stress $\overline{\sigma}_{2_1}$ is obtained (the subindex indicates the number of the sensor) acting on horizontal mortar joints; the measurements recorded by the sensor in position $[x^I_{2i}]$ which measure the horizontal displacement increasing monotonically $\overline{u}_{2n}$ (referred to the instant t_n). As output the measurements of the sensor LVDT3 in position x^O_{3i} are considered from which the horizontal force $\overline{F}_{3n}$ is obtained (see Fig. 6b).

Since the constitutive equations are expressed in terms of stress and deformation, the displacement $\bar{u}_{2n}$ is transformed into shear strain $\overline{\gamma}_{2n} = \overline{u}_{2n}/2s$ (s is the thickness of the mortar joint); while the horizontal force $\overline{F}_{3n}$ is replaced by the mean tangential stress $\overline{\tau}_{3n} = \overline{F}_{3n}/2A$ (A, area of the brick in contact with the mortar joint) acting on the joint in the ratio.

As *theoretical model* the constitutive equations in the functional form (6)–(8) are considered characterizing the three phases of the interface response in terms of tangential stress τ vs. shear strain γ. These equations are formulated in discrete terms, referring to the instant t_n, $\gamma_{2n} = f(\tau_{3n}, \underline{\theta})$, whereas they must be expressed as $\tau_{3n} = f(\gamma_{2n}, \underline{\theta})$ due to the softening branch in the experimental diagrams used as comparison elements in the objective function. To this end use is made of a procedure of polynomial interpolation in which for each experimental point $\overline{P}_n(\overline{\gamma}_{2n}, \overline{\tau}_{3n})$ two theoretical points are considered, $P_i(\gamma_i, \tau_i)$ and $P_{i+1}(\gamma_{i+1}, \tau_{i+1})$, such that $\gamma_i < \overline{\gamma}_{2n}$, $\gamma_{i+1} > \overline{\gamma}_{2n}$; thus the equation of the optimal curve crossing through the points P_i and P_{i+1} is determined and the position of the new point $P_n(\overline{\gamma}_{2n}, \widetilde{\tau}_{3n})$ is evaluated; this has as abscissa the experimental value $\overline{\gamma}_{2n}$ and as ordinate the value calculated with polynomial interpolation $\widetilde{\tau}_{3n}$. In the following the over-lining of the tangential stress will be omitted for simplicity of exposition ($\widetilde{\tau}_{3n} = \tau_{3n}$). This operation guarantees the correspondence on the abscissa of the theoretical measurements with the experimental ones.

The *objective function* Φ in the problem under consideration, as first application of the procedure, is based on the criterion (20) (remembering that in this criterion it is also necessary to insert the index m indicator of the test number):

$$\Phi(\underline{\theta}) = \sum_{m=1}^{M} \sum_{n=1}^{N} W_{m3n} e^2_{m3n}, \tag{23}$$

where the residual e_{m3n} is equal to

$$e_{m3n} = \overline{\tau}_{m3n} - \tau_{m3n}. \tag{24}$$

In (24) the experimental tangential stress $\overline{\tau}_{m3n}$ is measured by means of experimental tests on the triplet and compares with the corresponding theoretical measurement $\tau_{m3n} = f(\overline{\gamma}_{m2n}, \underline{\theta})$ evaluated through polynomial interpolation and calculated in correspondence with shear strain $\overline{\gamma}_{m2n}$ measured experimentally. The weight factors W_{m3n}, as explained in Section 4, are used to normalize the experimental data compared with $\overline{\tau}_{mr}$ value of maximum tangential stress of each single test or to subdivide the experimental curves into stretches of different weight. In the examples shown in the following part the former kind of weight factor is chosen.

With reference to the iterative procedure of optimal estimation proposed in Section 4, it is pointed out that the first attempt vector $\underline{\theta}_0$ is chosen in a domain limited by quantitative constraints of the elements of $\underline{\theta}$.

The result of every minimization iteration is calculated through (21), where the expression of the gradient turns out to be equal to

$$\underline{g}_k = \sum_{m=1}^{M} \sum_{n=1}^{N} \left(\frac{\partial \tau_{m3n}}{\partial \underline{\theta}} \right)^{\mathrm{T}} W_{m3n} e_{m3n} \Bigg|_{\underline{\theta}=\underline{\theta}_k}, \tag{25}$$

and the Gauss–Newton matrix is particularized in that

$$\widetilde{\underline{B}}_k = \sum_{m=1}^{M} \sum_{n=1}^{N} \left(\frac{\partial \tau_{m3n}}{\partial \underline{\theta}} \right)^{\mathrm{T}} W_{m3n} \left(\frac{\partial \tau_{m3n}}{\partial \underline{\theta}} \right) \Bigg|_{\underline{\theta}=\underline{\theta}_k}. \tag{26}$$

For calibration of the model two different approaches are followed: in Case 1 three tests are used in the identification process for each vertical stress; in Case 2, 12 tests for different vertical compression stresses are used simultaneously. The two cases must be considered suitable approaches with different aims, on the one hand (Case 1) one analyzes the effect of the variation of constant vertical stress σ_{2_1} on the response of the interface, on the other (Case 2) one seeks an instrument to estimate optimal parameters for the shear response of the material in presence of friction and cohesion.

Before commenting on the results obtained, one wishes to highlight the fact that a preliminary study was carried out (Morbiducci, 1998) in which estimates were made with *pseudo-experimental data* generated numerically and with single experimental curves of the shear triplet tests. In the first case the checks on the efficiency of the estimate procedure were carried out, in the second case it was decided to analyze the quality of the experimental data. From that study it came out that despite the good results of fitting of the single curves, the values of the estimates of unknown parameters are variables in the single estimates. These variations can be put down to the scattering of the experimental curves (in particular to the variation in the joint response in the softening phase) and to the dependence of the joint response on the imposed vertical compression.

In Table 3, the experimental data ($\overline{\sigma}_{2_i}$, number of experimental measures N), the identified parameters ($\underline{\hat{\theta}}$), the value of the final objective function ($\widehat{\Phi}$) and the corresponding variance are shown. Some examples of the numerical fitting obtained with the identified parameters are shown in Fig. 7. From the results obtained (see Table 3) a dependence of the parameter values to the normal compression acting on the joint was found, this dependence also found experimentally (Van Der Pluijm, 1993). Improvement of the mechanical characteristics of the joint with increase in compression (G_m, τ_m) is put down to the bordering effect of the bricks, whereas the decrease in the friction coefficient μ may be linked to the different modes of cracking of the sliding plane in relation to the vertical compression.

The variance of parameters in relation to the compression applied shows the necessity to carry out calibration of the local model by means of sufficient experimental information linked to this variance. Therefore one passed to Case 2 in which all the information available about shear response is inserted in a single estimation process. The results obtained are summarized in Fig. 8 and in Table 4 in which the mean

Table 3
Case 1

$\overline{\sigma}_{2_1}$ (MPa)	N	Iterations	$\widehat{\Phi}$	Variance	
0.12	513	26	2.32	0.004	
0.4	561	35	2.41	0.004	
0.8	621	42	2.19	0.003	
1.25	681	47	3.70	0.005	
	$\widehat{G}_m$ (MPa)	$\hat{c}_{mt}$ (mm^2/N)	$\hat{\mu}$	$\hat{\tau}_m$ (MPa)	$\hat{\beta}_m$
0.12	42.778	0.018	0.939	0.197	0.477
0.4	53.0190	0.0169	0.4460	0.3084	0.3670
0.8	86.7285	0.0330	0.2955	0.4729	0.3249
1.25	106.9400	0.0305	0.2022	0.6808	0.2757
	$G_m \rightarrow$	$c_{mt} \leftrightarrow$	$\mu \leftarrow$	$\tau_m \rightarrow$	$\beta_m \leftarrow$

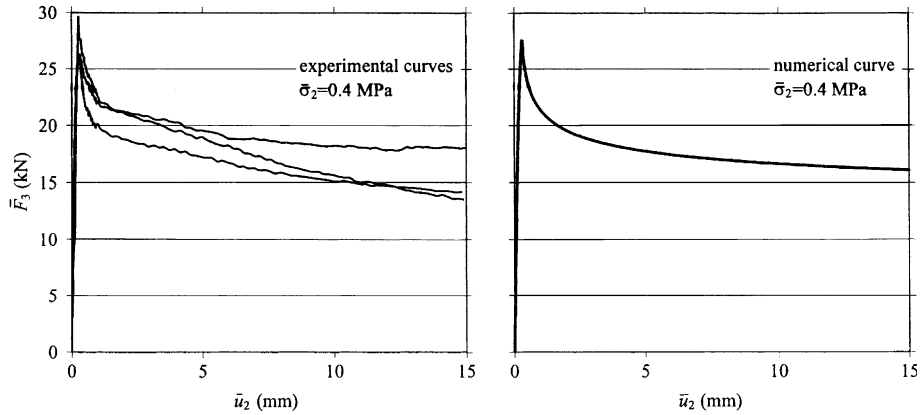

Fig. 7. Example of fitting of experimental data obtained from Case 1: $\overline{F}_{3n} = \overline{\tau}_{3n} 2A$, $\overline{u}_{2n} = \overline{\gamma}_{2n} 2s$.

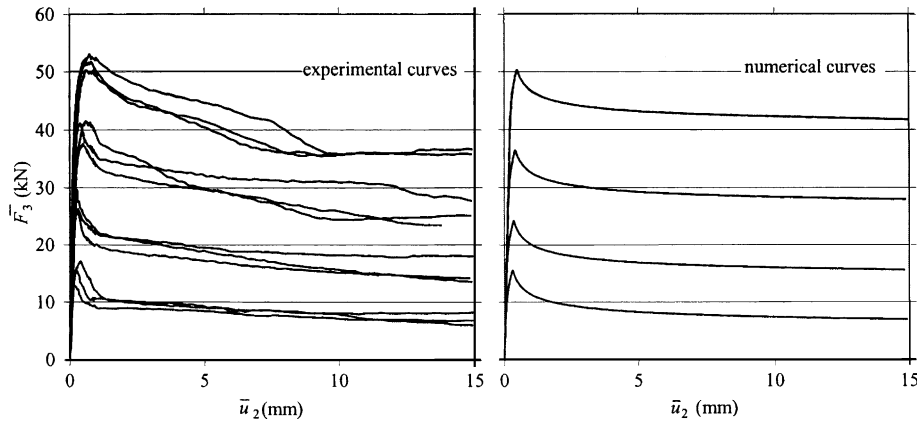

Fig. 8. Fitting of experimental data obtained from Case 2.

Table 4
Case 2

$\bar{\sigma}_{2_1}$ (MPa)	N	Iterations	$\widehat{\Phi}$	Variance	
0.12–1.25	2052	9	17.87	0.008	
	$\widehat{G}_m$ (MPa)	$\hat{c}_{mt}$ (mm^2/N)	$\hat{\mu}$	$\hat{\tau}_m$ (MPa)	$\hat{\beta}_m$
0.12-1.25	67.652	0.05	0.535	0.208	0.471
Average values Case 1	71.305	0.027	0.415	0.414	0.363

values of the estimated parameters in Case 1 are also shown; these turn out to be substantially different from the parameters estimated in Case 2.

In the identification problems the convergence of a minimization process is searched in a few iterations (see Tables 3 and 4). Control of the convergence of estimate processes is carried out following the two criteria described in Section 4.

5.2. Non-linear identification problem for damage continuum model

Direct calibration of the continuum model by means of global experimental tests (e.g. tests on masonry panels) in general is not permitted in that the information is not sufficient to determine the value of the single parameters, therefore it is necessary to use an implicit method. This may consist of the use of experimental test results on constituent materials and on small assemblages that allow one to indirectly trace the mean values of the unknown parameters through application of the homogenization technique. However, this type of process supplies very approximate values. The alternative approach is use of an identification method which allows estimation of the parameters by means of global experimental tests. In the case in consideration the damage continuum model is characterized by the following parameter vector, containing a high number of elements $\underline{\theta} = \{E_{M1}\ E_{M2}\ G_M\ \nu_{M12}\ \mu\ \sigma_m\ \tau_m\ \sigma_b\ \tau_b\ c_{mt}\ c_{bn}\ \beta_m\ \beta_b\}^{\mathrm{T}}$, thus one is dealing with resolving an identification problem in a high-dimensional parameter space.

The *experimental data* inserted in the identification processes refer to the tests carried out on masonry brick walls subjected to cyclic shear load superimposed on vertical compression (Anthoine et al., 1995, see Fig. 9a). The specimens are two different walls. The first (low wall) is 1 m wide and 1.35 m high, while the other is 2 m high (high wall). The wall thickness is 0.25 m. The masonry has English bond pattern brick unit size ($55 \times 120 \times 250$ mm) and 10 mm mortar joint thickness. These tests were carried out initially by

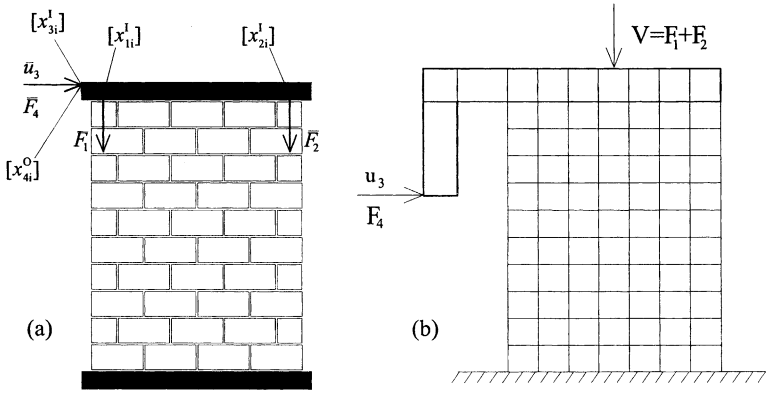

Fig. 9. Shear–compression testing of brick masonry walls: (a) test set-up; (b) finite element model of brick masonry walls.

applying a normal compressive stress of 0.6 MPa, then cyclic horizontal displacement with restrained rotation was imposed at the top.

Each estimation process considers as input data: the constant sum of the vertical forces $\overline{V} = \overline{F}_1 + \overline{F}_2$; these components are applied at the points corresponding to the sensors (1) and (2), (respectively in position $[x_{1i}^I]$ and $[x_{2i}^I]$), through a continuous rigid element and their sum is kept constant throughout the loading; the horizontal displacement $\bar{u}_{3n}$ measured in correspondence with the sensor (3) (identified by the position $[x_{3i}^I]$). Use of the two components of force $\overline{F}_1$ and $\overline{F}_2$ impedes the rotations that happen due to the effect of the horizontal displacements impressed. As output one considers the horizontal force $\overline{F}_{4n}$ obtained through the measurements of the sensor in position $[x_{4i}^O]$.

To apply the *continuum model* to the analysis of large scale shear walls having general shape, a finite element procedure is used based on the plane stress assumption for the wall. Four-node finite isoparametric elements are used. The dimensions of the finite element (143×135 mm) are chosen taking into account the position in height of the mortar joints, which are the elements with the greatest weakness. In particular the finite elements size is selected to obtain a direct correspondence between a Gauss point and a mortar bed joint, while a no rigorous criterion is used to define the element width, that is a Gauss point is related to a portion of mortar bed joint included between two adjacent mortar head joints (for more details see Gambarotta and Lagomarsino, 1997b). To reproduce the boundary conditions of the experimental tests the model of Fig. 10b is adopted. The mesh is made up of 70 elements (98 for the high wall). The load conditions foresee a first step in which the constant vertical load is imposed and a successive series of increases of cyclic horizontal displacements N (low wall, $N = 120$; high wall, $N = 155$) imposed on the nodes of the rigid element indicated in the figure until the maximum displacement is reached (low wall, $u_2 = 8$ mm; high wall, $u_2 = 12.5$ mm). The points of application of the imposed displacements enable reproduction of the loading conditions of the simulated experimental test. The applied lateral deflection step u_{3n} and the corresponding horizontal force F_{4n}, are the quantities of comparison respectively of the experimental measurements $\overline{u}_{3n}$ and $\overline{F}_{4n}$ present in the objective function.

It is again preferred to use an estimation criterion (20) to be able to analyze the feasibility of the proposed procedure for the non-holonomic model calibration, rather than carrying out studies of the influence of uncertainties. The objective function Φ assumes the following form, in that every estimation process use data from a single test:

$$\Phi(\underline{\theta}) = \sum_{n=1}^{N} W_{4n} e_{4n}^2, \tag{27}$$

where the residual e_{4n} is equal to

$$e_{4n} = \overline{F}_{4n} - F_{4n}, \tag{28}$$

W_{4n} is the weight factor inserted to normalize the measurements compared in the objective function with respect to $\overline{F}_{\max}$ (maximum value reached by the horizontal force). This is the simplest choice for a weight factor, it solves the problem to sum squares of different orders of magnitude. Besides there are not information about different reliable of observation, thus it is assumed that every observation has the same weight.

The minimization process of (27) is based on the same numerical-iterative procedure used for calibration of the interface model. This is possible in that use of such procedure (schematized in Fig. 5) requires definition and imposition of the minimum condition of a function depending on the parameters to be estimated. This operation is possible even in the case of calibration of the continuum model. The procedure is generalized in order to use cyclic load histories and to insert a program for resolution of a numeric-discrete problem as external element to the same procedure (e.g. finite element program). This

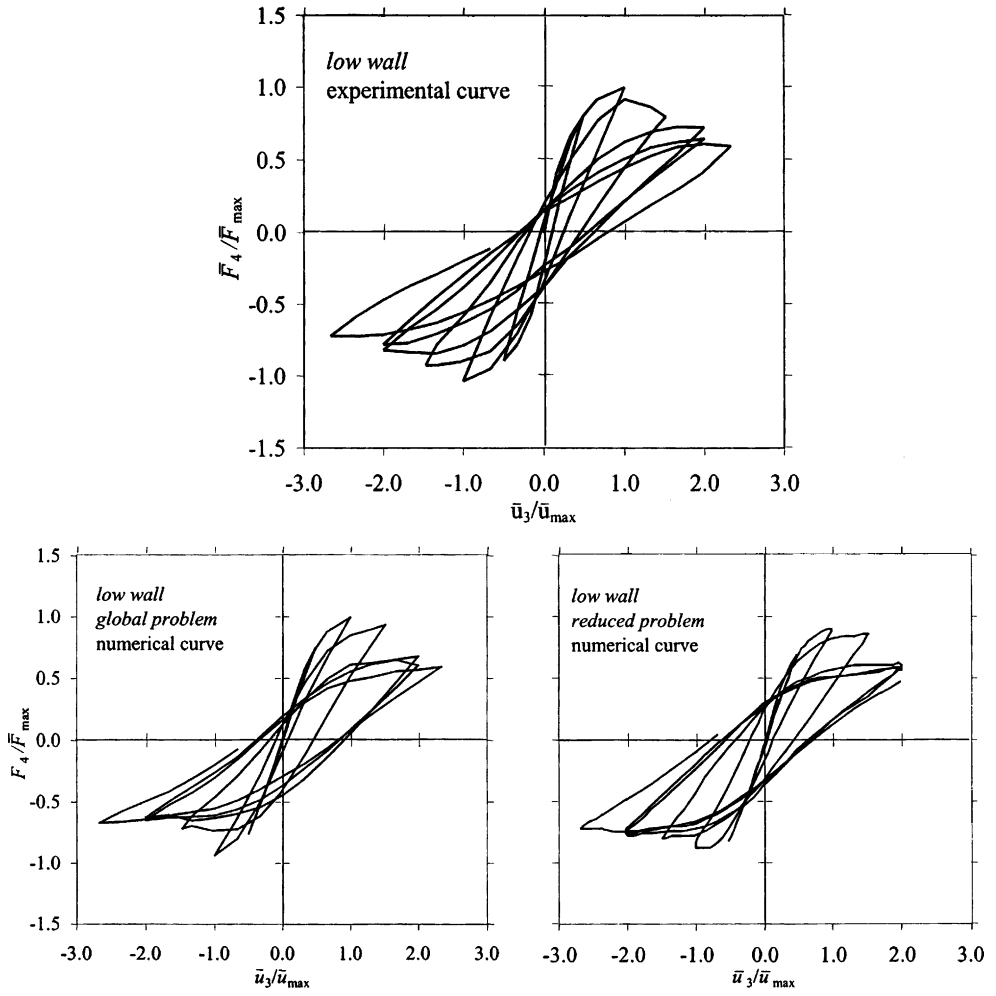

Fig. 10. Example of fitting of experimental data in the identification problem for damage continuum model: low wall.

generalization made the estimation method flexible and applicable to different theoretical models (Morbiducci and Shing, 1998; Morbiducci et al., 1999).

The estimation problem studied here is characterized by the necessity to adopt a finite element discretization of the continuum model to evaluate the force components and to insert them as comparison quantities with the corresponding experimental measurements. This means that for every iteration of the minimization process it is necessary to carry out a finite element analysis to define the objective function Φ and P finite element analyzes to calculate the partial numerical derivatives (with respect to P unknown parameters) for the gradient $\underline{g}_k$ and the Gauss–Newton matrix $\underline{\widetilde{B}}_k$ of the objective function.

Two different approaches to estimate the elements of $\underline{\theta}$ are followed, the first is known as the *global problem* in which the entire parameter vector is estimated; in this case one disregards the possibility of deducing some parameters from local tests. The second approach is classified as the *reduced problem*, in that only some elements of the parameter vector are assumed as unknowns of the identification process. In particular G_M, τ_m, σ_b, c_{mt}, c_{bn}, β_m and β_b are introduced as elements of the vector to be identified, given the

type of test used and given the minor uncertainty in determining certain parameters. In the reduced problem the elements of $\underline{\theta}$ that are not inserted in the calibration process are deduced from local experimental tests and from the results of identification processes for the interface model. The reduced problem is a case of non-linear calibration in which the unknown parameter vector $\underline{\theta}$ and the known parameter vector $\underline{b}$ must be distinguished. In the following, some results obtained are shown considering the two different geometry of the panels.

In Tables 5 and 6 the results obtained in the global problem are summarized in terms of the experimental data ($\overline{\sigma}_{2_i}$, number of experimental measures N), the identified parameters ($\hat{\underline{\theta}}$), the value of the final objective function ($\widehat{\Phi}$) and the corresponding variance. Convergence in the estimation process is reached taking account of the quantitative constraints on parameters, necessary to ensure their physical significance. The quality of the estimate is good in terms of a posteriori variance. In order to reduce the number of iterations the feasibility of the reduced problem is checked. In this case the number of unknown parameters is halved, $\underline{\theta} = \{G_M \ \tau_m \ \sigma_b \ c_{mt} \ c_{bn} \ \beta_m \ \beta_b\}^{\mathrm{T}}$, $\underline{b} = \{E_{M1} \ E_{M2} \ \nu_{M12} \ \mu \ \sigma_m \ \tau_b\}^{\mathrm{T}}$. The elements of $\underline{b}$, except μ, are implicitly deduced from local experimental tests; whereas the friction coefficient μ is assumed equal to the value

Table 5
Global problem, low wall

Nodes	Elements	Load steps	Iterations	$\widehat{\Phi}$	Variance	
102	80	121	25	1.255	0.01	
$\widehat{E}_{M1}$ (MPa)	$\widehat{E}_{M2}$ (MPa)	$\hat{\nu}_{12}$	$\widehat{G}_M$ (MPa)	$\hat{\mu}$	$\hat{\sigma}_m$ (MPa)	$\hat{\tau}_m$ (MPa)
2500	1800	0.192	531	0.6	0.1	0.34
$1/\hat{c}_{mt}$ (MPa)	$\hat{\beta}_m$	$\hat{\sigma}_b$ (MPa)	$\hat{\tau}_b$ (MPa)	$1/\hat{c}_{bn}$ (MPa)	$\hat{\beta}_b$	
1097	0.8	4.8	1.3	1087	0.24	

Table 6
Global problem, high wall

Nodes	Elements	N	Iterations	$\widehat{\Phi}$	Variance	
118	108	155	22	1.178	0.008	
$\widehat{E}_{M1}$ (MPa)	$\widehat{E}_{M2}$ (MPa)	$\hat{\nu}_{12}$	$\widehat{G}_M$ (MPa)	$\hat{\mu}$	$\hat{\sigma}_m$ (MPa)	$\hat{\tau}_m$ (MPa)
2200	1700	0.189	541	0.58	0.15	0.35
$1/\hat{c}_{mt}$ (MPa)	$\hat{\beta}_m$	$\hat{\sigma}_b$ (MPa)	$\hat{\tau}_b$ (MPa)	$1/\hat{c}_{bn}$ (MPa)	$\hat{\beta}_b$	
986	0.9	4.9	1.2	1053	0.22	

Table 7
Reduced problem, low wall

Nodes	Elements	Load steps	Iterations	$\widehat{\Phi}$	Variance	
124	108	121	18	1.4166	0.01	
$\widehat{G}_M$ (MPa)	$\hat{\tau}_m$ (MPa)	$1/\hat{c}_{mt}$ (MPa)	$\hat{\beta}_m$	$\hat{\sigma}_b$ (MPa)	$1/\hat{c}_{bn}$ (MPa)	$\hat{\beta}_b$
1439	0.4	763	1	5.6	1145	0.2
Known parameters ($\underline{b}$)						
E_{M1} (MPa)	E_{M2} (MPa)	ν_{12}	μ	σ_m (MPa)	τ_b (MPa)	
1910	1480	0.26	0.54	0.05	5.9	

identified by means of the estimation processes of the interface model. From a comparison of the results obtained with the two different approaches (see Tables 7 and 8, Figs. 10 and 11) it can be seen that the quality of the estimate in the reduced problem is slightly less in terms of a posteriori variance, but the saving

Table 8
Reduced problem, high wall

Nodes	Elements	N	Iterations	$\widehat{\Phi}$	Variance	
118	108	155	13	1.1946	0.008	
$\widehat{G}_M$ (MPa)	$\hat{\tau}_m$ (MPa)	$1/\hat{c}_{mt}$ (MPa)	$\hat{\beta}_m$	$\hat{\sigma}_b$ (MPa)	$1/\hat{c}_{bn}$ (MPa)	$\hat{\beta}_b$
850	0.45	650	0.8	5.0	1000	0.1
Known parameters ($\underline{b}$)						
E_{M1} (MPa)	E_{M2} (MPa)	ν_{12}	μ	σ_m (MPa)	τ_b (MPa)	
1910	1480	0.26	0.54	0.05	5.9	

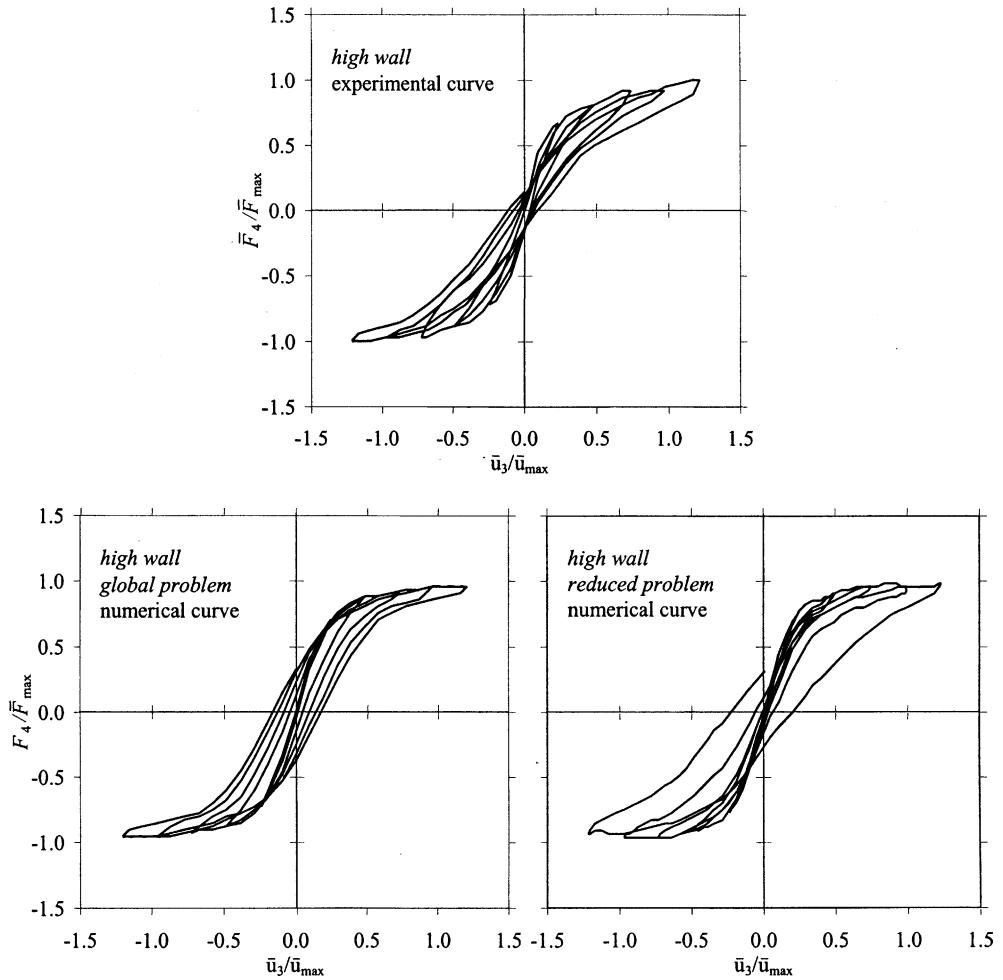

Fig. 11. Example of fitting of experimental data in the identification problem for damage continuum model: high wall.

in calculation times is considerable. In fact the number of finite element analyzes in each estimate iteration is halved and moreover the number of iteration comes down.

6. Conclusions

In this work a generalization of the indirect calibration problem of constitutive models has been proposed analyzing the meaning and role of the elements that make up a parameter identification process.

An indirect calibration procedure is proposed in which the estimate method is chosen on the basis of information on the uncertainties of known parameters of constitutive model and/or information on errors of experimental measurements. The minimization process of the discrepancies between experimental and theoretical measurements is based on a method of Levenberg–Marquardt characterized by use of the Gauss–Newton matrix as a simplified Hessian matrix. The procedure is applicable for calibration of models in holonomic and non-holonomic form. The experimental data compared with the theoretical measurements can be monotonic or cyclic and more runs of the same experimental test can be considered.

In this work as first application of the numerical procedure the following estimates were carried out: estimation of the unknown parameters of an interface model (in functional form) by means of monotonic experimental test data; parameter identification of a continuum model (in non-holonomic form) for brick masonry by means of cyclic experimental data.

The results obtained confirm the possibility of calibrating the two models by means of the experimental tests chosen. In the case of the interface model the necessity to use experimental tests in which the compression acting on the joint is made to vary is found. In the case of the continuum model two different approaches to estimate the unknown parameters are analyzed, the global problem and the reduced problem. The latter involved a considerable reduction of numerical iterations with a small reduction of the estimate quality.

References

Aktinson, R.H., Amadei, P.B., Saeb, S., Sture, S., 1989. Response of masonry bed joints in direct shear. J. Struct. Engng., ASCE 115 (9), 2276–2296.

Anthoine, A., 1995. Derivation of in-plane elastic characteristics of masonry through homogenization theory. Int. J. Solids Struct. 32 (2), 137–163.

Anthoine, A., Magenes, G., Magonette, G., 1995. Shear–compression testing and analysis of brick masonry walls. In: Duma, G. (Ed.), Proceedings of 10th European Conference on Earthquake Engineering, vol. 3. Balkema, Rotterdam, pp. 1657–1662.

Bard, Y., 1974. Nonlinear Parameter Estimation. Academic Press, New York, USA.

Binda, L., Mirabella Roberti, G., Tiraboschi, C., Abbaneo, S., 1994. Measuring masonry material properties. In: Proceedings of US–Italy Workshop on Guidelines for Seismic Evaluation and Rehabilitation of Unreinforced Masonry Buildings, NCEER-94-0021, Buffalo, NY, pp. 6.3–6.24.

Fadale, T.D., Nenarokomov, A.V., Emery, A.F., 1995. Uncertainties in parameter estimation: the inverse problem. Int. J. Heat Mass Transfer 38 (3), 511–518.

Federov, V.V., Hackl, P., 1997. Model-oriented Design of Experiments. In: Lecture Notes in Statistics, vol. 125. Springer-Verlag, NY.

Gambarotta, L., Lagomarsino, S., 1997a. Damage models for seismic response of brick masonry shear walls. Part I: the mortar joint model and its applications. Earthquake Engng. Struct. Dyn. 26, 423–439.

Gambarotta, L., Lagomarsino, S., 1997b. Damage models for seismic response of brick masonry shear walls. Part II: the continuum model and its applications. Earthquake Engng. Struct. Dyn. 26, 441–462.

Lofti, H.R., Shing, P.B., 1994. Interface model applied to fracture of masonry structures. ASCE, J. Struct. Engng. 120 (1), 63–80.

Lourenço, P.B., Rots, J.G., 1997. Multisurface interface model for analysis of Masonry structures. ASCE, J. Engng. Mech. 123 (7), 660–668.

Lourenço, P.B., Rots, J.G., Blaauwendraad, J., 1998. Continuum model for Masonry: parameter estimation and validation. ASCE, J. Struct. Engng. 124 (6), 642–652.

Luciano, R., Sacco, E., 1997. Homogenization technique and damage model for old masonry material. Int. J. Solids Struct. 34 (24), 3191–3208.

Luenberg, D.G., 1989. Linear and Nonlinear Programming. Addison-Wesley Publishing Company, Reading, MA, USA.

Manzouri, T., Shing, P.B., Amedei, B., Shuller, M.P., Atkinson, R.H., 1995. Repair and retrofit of unreinforced masonry walls: experimental evaluation and finite element analysis. Report No. CU/SR-95/2, Department of Civil, Environmental, and Architectural Engineering, University of Colorado, Boulder, CO, USA.

Morbiducci, R., 1998. Comportamento non lineare della muratura: modelli costitutivi, risultati sperimentali ed identificazione parametrica. Ph.D. Thesis, Politecnico of Milan, Italy.

Morbiducci, R., Shing, P.B., 1998. Parameter identification of a nonlinear interface model for masonry mortar joints. In: Tanaka, M., Dulikravich, G.S. (Eds.), Proceedings of Inverse Problem in Engineering Mechanics. Elsevier Science, Nagano, Japan, pp. 273–282.

Morbiducci, R., Papa, E., Nappi, A., 1999. Identificazione parametrica di modelli al continuo per pareti in muratura. In: Proceedings of XIV Congresso Nazionale dell'Associazione Italiana di Meccanica Teorica ed Applicata, Italy.

Pande, G.N., Liang, J.X., Middleton, J., 1989. Equivalent elastic moduli for brick masonry. Comput. Geotech. 8, 243–265.

Papa, E., 1996. A unilateral damage model for masonry based on a homogenization procedure. Mech. Cohes.-Frict. Mater. 1, 349–366.

Press, W.H., Teukolsky, S.A., Vetterling, W.T., Flannery, B.P., 1992. Numerical Recipes in Fortran. The Art of Scientific Computing, second ed Cambridge University Press, NY, USA.

Sorenson, H.W., 1980. Parameter Estimation: Principles and Problems. Marcel Dekker, New York.

Van Der Pluijm, R., 1993. Shear behavior of brick masonry under combined shear and compression loading. In: Proceedings of Sixth North American Masonry Conference, vol. 1, Philadelphia, pp. 125–136.